

This article was downloaded by:

On: 25 January 2011

Access details: *Access Details: Free Access*

Publisher *Taylor & Francis*

Informa Ltd Registered in England and Wales Registered Number: 1072954 Registered office: Mortimer House, 37-41 Mortimer Street, London W1T 3JH, UK



## Separation Science and Technology

Publication details, including instructions for authors and subscription information:

<http://www.informaworld.com/smpp/title~content=t713708471>

### Chemical Absorption of Carbon Dioxide into Aqueous Solution of Potassium Threonate

Kyu-Suk Hwang<sup>a</sup>; Dae-Won Park<sup>a</sup>; Kwang-Joong Oh<sup>a</sup>; Seong-Soo Kim<sup>b</sup>; Sang-Wook Park<sup>a</sup>

<sup>a</sup> School of Chemical and Biomolecular Engineering, Pusan National University, Busan, Korea <sup>b</sup>

Department of Environmental Administration, Catholic University of Pusan, Busan, Korea

Online publication date: 22 February 2010

**To cite this Article** Hwang, Kyu-Suk , Park, Dae-Won , Oh, Kwang-Joong , Kim, Seong-Soo and Park, Sang-Wook(2010) 'Chemical Absorption of Carbon Dioxide into Aqueous Solution of Potassium Threonate', *Separation Science and Technology*, 45: 4, 497 – 507

**To link to this Article:** DOI: [10.1080/01496390903529919](https://doi.org/10.1080/01496390903529919)

URL: <http://dx.doi.org/10.1080/01496390903529919>

## PLEASE SCROLL DOWN FOR ARTICLE

Full terms and conditions of use: <http://www.informaworld.com/terms-and-conditions-of-access.pdf>

This article may be used for research, teaching and private study purposes. Any substantial or systematic reproduction, re-distribution, re-selling, loan or sub-licensing, systematic supply or distribution in any form to anyone is expressly forbidden.

The publisher does not give any warranty express or implied or make any representation that the contents will be complete or accurate or up to date. The accuracy of any instructions, formulae and drug doses should be independently verified with primary sources. The publisher shall not be liable for any loss, actions, claims, proceedings, demand or costs or damages whatsoever or howsoever caused arising directly or indirectly in connection with or arising out of the use of this material.

# Chemical Absorption of Carbon Dioxide into Aqueous Solution of Potassium Threonate

Kyu-Suk Hwang,<sup>1</sup> Dae-Won Park,<sup>1</sup> Kwang-Joong Oh,<sup>1</sup> Seong-Soo Kim,<sup>2</sup> and Sang-Wook Park<sup>1</sup>

<sup>1</sup>*School of Chemical and Biomolecular Engineering, Pusan National University, Busan, Korea*

<sup>2</sup>*Department of Environmental Administration, Catholic University of Pusan, Busan, Korea*

**Carbon dioxide was absorbed into aqueous solution of potassium threonate (PT) at different concentrations of PT and CO<sub>2</sub>, and temperatures in the range of 0.1–1.0 kmol/m<sup>3</sup>, 10.1–101.3 kPa, and 293–313 K, respectively, using a stirred semi-batch vessel with a planar gas-liquid interface. Both the reaction order and rate constant were determined from gas absorption rates under the fast pseudo-first-reaction regime. The reaction was found to be first order with respect to both CO<sub>2</sub> and PT, and its activation energy has been found to be 40.6 kJ/mol. From a comparison of the reaction kinetics by the overall reaction scheme with those by the elementary reaction scheme based on the zwitterions mechanism, the overall reaction between CO<sub>2</sub> and PT has been found to be equivalent to the formation of zwitterions.**

**Keywords** absorption; carbon dioxide; potassium threonate

## INTRODUCTION

Carbon dioxide in the flue gas generated as a result of combustion of fossil fuel in thermal power plants, etc., is the main cause of global environmental problems such as the global warming and acid rain. One of the conventional methods to achieve the removal and recovery of CO<sub>2</sub> on an industrial scale is the chemical absorption method. One important requirement involved with this method is to develop absorbents with high absorption rate and capacity. Industrially important chemical absorbents are alkanolamines (1–4). However, alkanolamine easily degrade, especially in oxygenated environments, making necessary the developments of new absorbents for gas mixtures with significant oxygen concentrations, namely for flue gas, life support systems and anesthetic gas circuits (5). Alkali salts of amino acids have the same functional group as alkanolamines (presenting similar capacities and reaction rates with CO<sub>2</sub>) and are much more stable in the presence of oxygen (6). Besides, due to the ionic nature of the solutions,

they present lower volatilities and higher surface tensions (7). They are reported to be used for the selective removal of acid gases in some industrial processes (8) as a new absorbent for CO<sub>2</sub> absorption. Many studies have been done towards the mechanisms and kinetics of the reaction of CO<sub>2</sub> with various alkanolamines (8), whereas data about reaction kinetics of CO<sub>2</sub> with salts of amino acid are still scarce (5–7,9–12). They generally used the overall reaction kinetics to obtain the reaction rate constant in the reaction between CO<sub>2</sub> and salt of amino acid under an assumed pseudo-first order reaction. They did not observe the kinetics of the elementary reactions using the zwitterion mechanism proposed by Danckwerts (13), the reaction order with respect to both CO<sub>2</sub> and amino acid salt. Because the diffusion may have an effect on the reaction kinetics (14) in the mass transfer accompanied by chemical reactions, we believe it worthwhile to investigate this effect on the reaction kinetics of the gas-liquid heterogeneous reaction between CO<sub>2</sub> and amino salt.

To our knowledge, no literature report about absorption kinetics using salts of amino acids to absorb CO<sub>2</sub> has yet been published except the articles as mentioned above (5–7,9–12), which have been chiefly described to obtain the overall reaction kinetics between CO<sub>2</sub> and amino acid salts, or to measure the solubility and diffusivity of CO<sub>2</sub> in amino acid salts. Portugal et al. (5) obtained the overall kinetic constant of Arrhenius type with potassium threonate (PT) concentration using the measured rate of CO<sub>2</sub> into aqueous solution of PT in a closed absorber under fast pseudo-first-order reaction regime. In this paper, the experimental data about the absorption of CO<sub>2</sub> into aqueous solution of PT are measured by changing the partial pressure of CO<sub>2</sub> and concentration of PT at 293–313 K. These data are analyzed to investigate the reaction kinetics between CO<sub>2</sub> and PT using two reaction schemes of the overall reaction scheme and elementary reaction scheme. The one is for the reaction rate constant and the reaction orders with respect to CO<sub>2</sub> and PT, the other for confirmation of the rate-determining step based on the zwitterions

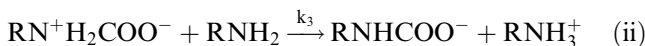
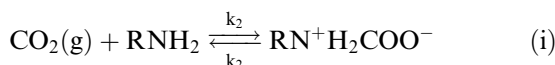
Received 2 September 2009; accepted 10 November 2009.

Address correspondence to Sang-Wook Park, School of Chemical and Biomolecular Engineering, Pusan National University, Busan 609-735, Korea. E-mail: swpark@pusan.ac.kr

mechanism. Solubility of  $\text{CO}_2$  and diffusivity of  $\text{CO}_2$  and PT, which are necessary to obtain the reaction kinetics, were used from the data by Portugal et al. (5).

## THEORY

In case of  $\text{CO}_2$  absorption into aqueous solution containing primary and secondary amines, the zwitterions mechanism originally proposed by Caplow (15) and reintroduced by Danckwerts (13) and da Silva and Svendsen (16) is generally accepted to occur in two steps as follows:



where R presents  $-\text{C}(-\text{OH})\text{H}-\text{CH}_3\text{H}-\text{C}(=\text{O})-\text{OK}$ .

It has been reported (6) that the first step, the formation of zwitterions, in above two steps, is bimolecular, second-order and hence the rate-determining step, while the second step is supposed to take place instantaneously.

The overall reaction between  $\text{CO}_2$  and PT is given by



Reaction (iii) may be formulated as follows:



where  $\nu_A$  is a stoichiometric coefficient of species A and assumed to be 1 according to reaction (iii) because of the instantaneous reaction of reaction (ii).

## Overall Reaction Scheme

To obtain the overall reaction kinetics of reaction (iv), the following assumptions (11) are made to set up the mass balance of species A and B:

1. Henry's law holds,
2. isothermal condition prevails,
3. species B is a nonvolatile solute,
4. the gas-phase resistance to gas absorption is negligible, and
5. reaction (iv) is mth order with respect to A and nth order with respect to B, of which the reaction rate ( $r_{A,\text{overall}}$ ) is expressed by

$$r_{A,\text{overall}} = k C_A^m C_B^n \quad (\text{v})$$

The mass balances of species A and B in the film liquid based on the film theory accompanied by reaction (v) and the boundary conditions are given as follows:

$$D_A \frac{d^2 C_A}{dz^2} = r_{A,\text{overall}} \quad (\text{1})$$

$$D_B \frac{d^2 C_B}{dz^2} = \nu_A r_{A,\text{overall}} \quad (\text{2})$$

$$z = 0; \quad C_A = C_{Ai}, \quad \frac{dC_B}{dz} = 0 \quad (\text{3})$$

$$z = \delta; \quad C_A = 0, \quad C_B = C_{Bo} \quad (\text{4})$$

The molar flux of species A at the gas-liquid interface phase is defined by

$$N_A = -D_A \left( \frac{dC_A}{dz} \right)_{z=0} \quad (\text{5})$$

Although not only the physicochemical properties, but the values of m and n should be given to obtain the theoretical  $N_A$  of Eq. (5), but, for convenience' sake, the systems, classified into four regimes such as very slow reaction, slow reaction, fast reaction, and instantaneous reaction (14) depending on the relative rates of diffusion and reaction, have been used.

The condition for validity of fast pseudo-mth-order reaction with respect to species A, where the interfacial concentration of species B is the same as that in the bulk liquid phase, is given by the following expression (16):

$$1 < \text{Hatta} \ll E_i \quad (\text{6})$$

where

$$\text{Hatta} = \frac{\sqrt{\frac{2}{m+1}} D_A k C_{Ai}^{m-1} C_{Bo}^n}{k_L} \quad (\text{7})$$

$$E_i = \sqrt{\frac{D_A}{D_B}} + \frac{C_{Bo}}{\nu_A C_{Ai}} \sqrt{\frac{D_A}{D_B}} \quad (\text{8})$$

$E_i$  is defined as the instantaneous reaction enhancement factor and is derived from the penetration theory, since the experimental data of the absorption rates are better correlated through use of  $(D_A/D_B)^{0.5}$  than  $D_A/D_B$  (14).

If Eq. (6) is satisfied, Eq. (1) can be written as

$$D_A \frac{d^2 C_A}{dz^2} = k C_A^m C_{Bo}^n = k_m C_A^m \quad (\text{9})$$

where

$$k_m = k C_{Bo}^n \quad (\text{10})$$

Using the solution of Eq. (9) with the boundary conditions of Eqs. (3) and (4),  $N_A$  of Eq. (5) is derived as follows:

$$N_A = C_{Ai} \sqrt{\frac{2}{m+1}} D_A k C_{Ai}^{m-1} C_{Bo}^n \quad (\text{11})$$

Equation (11) shows that  $N_A$  is independent of  $k_L$ , that is, the hydrodynamics of the stirred semi-batch tank with a planar gas-liquid interface.

Where the resistance in the gas phase is not negligible, the expression for  $N_A$  for the pseudo-mth order regime is derived as follows:

$$\frac{P_A}{N_A} = \frac{1}{k_G} + \frac{H_A}{\sqrt{\frac{2}{m+1} D_A k C_{Ai}^{m-1} C_{Bo}^n}} \quad (12)$$

For negligible resistance in the gas phase, plots of  $P_A/N_A$  vs.  $H_A/(D_A k C_{Bo})^{0.5}$  at constant temperature should, according to Eq. (12), be a straight line passing through the origin with slope of 1 for  $m=n=1$ .

### Elementary Reaction Scheme

To obtain the elementary reaction kinetics of reaction (i) and (ii) based on the zwitterions mechanism, the steady state approximation is applied to the zwitterions, and then, one gets a rate of homogeneous reaction as

$$r_{A,elemen} = \frac{C_A C_B}{\frac{1}{k_1} + \frac{k_2}{k_1 k_3 C_B}} \quad (13)$$

The mass balances of species A and B in the film liquid based on the film theory accompanied by reaction (i) and (ii) are given as follows:

$$D_A \frac{d^2 C_A}{dz^2} = r_{A,elemen} \quad (14)$$

$$D_B \frac{d^2 C_B}{dz^2} = \nu_A r_{A,elemen} \quad (15)$$

The boundary conditions are given in Eqs. (3) and (4).

If the absorption process is conducted under conditions where the liquid phase reaction may be considered first-order with respect to  $\text{CO}_2$  (14), the rate of reaction for  $\text{CO}_2$  will be given as follows:

$$r_{A1} = k_o C_A \quad (16)$$

where  $k_o$  is derived from Eqs. (13) and (16) as

$$k_o = \frac{C_{Bo}}{\frac{1}{k_1} + \frac{k_2}{k_1 k_3 C_{Bo}}} \quad (17)$$

The material balance equation based on the film theory and the boundary conditions can be written as

$$D_A \frac{d^2 C_A}{dz^2} = r_{A1} \quad (18)$$

$$z = 0, \quad C_A = C_{Ai} \quad (19)$$

$$z = z_L, \quad C_A = 0 \quad (20)$$

Using the molar flux ( $N_A$ ) of A at interface of gas and liquid ( $-D_A dC_A/dz$ ), which is obtained from the exact solution of Eq. (18), and the physical molar flux ( $N_{Ao}$ ), the enhancement factor ( $\beta$ ) here defined as the ratio of molar flux with chemical reaction to that without chemical reaction ( $N_A/N_{Ao}$ ) is described as follows:

$$\beta = \frac{M}{\tanh M} \quad (21)$$

where  $M^2 = k_o D_A / k_L^2$ .

Equation (21) gives the value of  $k_o$  using the experimental value ( $\beta_{exp}$ ) of  $\beta$ . The values of  $k_1$  and  $k_2/k_3$  are determined using Eq. (22), rearranged from Eq. (17), through a plot of the left-hand side of Eq. (22) vs.  $1/C_{Bo}$ .

$$\frac{C_{Bo}}{k_o} = \frac{1}{k_1} + \frac{k_2}{k_1 k_3 C_{Bo}} \quad (22)$$

## EXPERIMENTAL

### Chemicals

All chemicals were of reagent grade, and used without further purification. Purity of  $\text{CO}_2$ , and  $\text{N}_2$  were more than 99.9%. The potassium threonate aqueous solutions were prepared, along the procedure similar to that reported elsewhere (7), by neutralizing the amino acid (threonine, 98% purity, Aldrich), dissolved in deionized distilled water, with an equimolar quantity of KOH (Alrich) in a standard flask. The neutralization reaction was carried out with constant cooling. The amino acid dissolved in water exists as a zwitterions, with the amino group completely protonated. The concentration of the protonated amine (amino acid salt) was estimated potentiometrically, by titrating with standard HCl solutions.

### Absorption Rate of $\text{CO}_2$

Absorption apparatus used to measure the absorption rate of  $\text{CO}_2$  is shown in Fig. 1, which is similar to that reported elsewhere (4,17). The absorption vessel was constructed of glass of 0.073 m in inside diameter and of 0.151 m in height. Four equally spaced vertical baffles, each one-tenth of the vessel diameter in width, were attached to the internal wall of the vessel. The gas and liquid phase were agitated with an agitator driven by a 1/4 Hp variable speed motor. Two straight impellers with 0.034 m in length and 0.05 m in width were used as the agitators in gas and liquid phase, respectively, which were agitated at the middle position of the each phase with the agitation speed of 50 rpm. The surface area of the liquid was measured and its value was  $4.10 \times 10^{-3} \text{ m}^2$ . The value of the cumulative volume of the soap bubble was measured by a soap

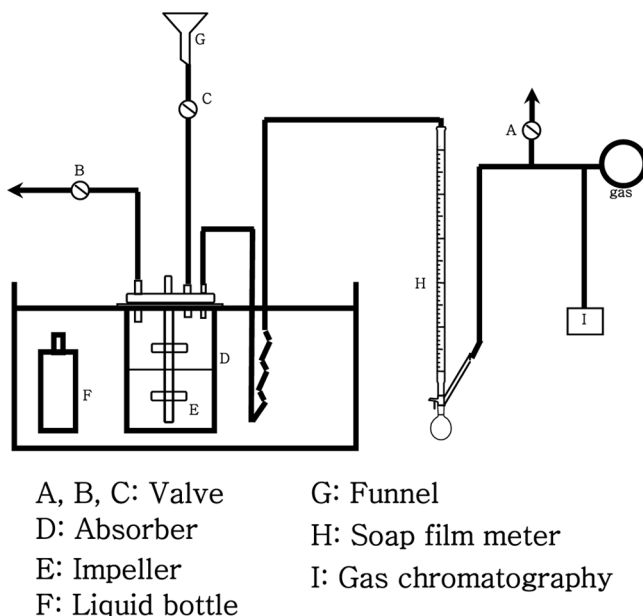


FIG. 1. Schematic diagram of the agitated vessel.

bubbler for the change of absorption time to obtain the absorption rate of  $\text{CO}_2$ . It was assumed that the volumetric rising rate of the soap bubble in the soap bubbler attached to the absorption vessel was equal to the value of absorption rate of  $\text{CO}_2$ . The measured molar flux of  $\text{CO}_2$  ( $N_{A,\text{exp}}$ )

was obtained using the absorption rate and the surface area of the liquid. The absorption experiments were carried out in the range of 0.3–1.0  $\text{kmol}/\text{m}^3$  of PT, 1.013–10.13 kPa of  $\text{CO}_2$  partial pressure, and 298–313 K along the procedure similar to those reported elsewhere (4,17).

### Physical Properties

The nitrous oxide analogy (5,18,19) has been used to approximate diffusivity and Henry's constant of gas species in aqueous solution. Portugal et al. (5) have measured diffusivity and Henry's constant ( $H_A$ ) of  $\text{CO}_2$  in PT aqueous solution of 0.1–3.0  $\text{kmol}/\text{m}^3$  and 293–313 K using  $\text{N}_2\text{O}$  analogy.

Because amino acid salt solutions are ionic in nature, a salting-out effect needs to be taken into account when interpreting the solubility data of gases in these solutions. At moderately high salt concentrations, this effect can be accounted for using the Sechenov relation (20):

$$\log\left(\frac{H_A}{H_{AW}}\right) = K_A C_B \quad (23)$$

where  $K_A$  is the Sechenov constant, which is estimated by the  $\text{N}_2\text{O}$  analogy (5) as follows:

$$K_A = h_+ + h_- + 2h_A \quad (24)$$

TABLE 1  
Absorption data for various  $C_{\text{Bo}}$  and  $P_A$  at 293 K

$P_A \times 10^{-2}$ (Pa)	$C_{\text{Bo}}$ ( $\text{kmol}/\text{m}^3$ )	$\mu \times 10^3$ (kg/ms)	$C_{\text{Ai}} \times 10^4$ ( $\text{kmol}/\text{m}^3$ )	$N_{A,\text{exp}} \times 10^7$ ( $\text{kmol}/\text{m}^2\text{s}$ )	Hatta	$E_i$
10.13	0.3	1.132	3.48	1.16	22	659
	0.5	1.234	3.27	1.31	29	1178
	0.8	1.391	2.97	1.44	37	2095
	1.0	1.509	2.79	1.46	42	2811
30.39	0.3	1.132	10.44	3.35	7	220
	0.5	1.234	9.81	3.93	10	394
	0.8	1.391	8.92	4.32	12	699
	1.0	1.509	8.38	4.39	14	938
50.65	0.3	1.132	17.41	5.58	4	133
	0.5	1.234	16.35	6.55	6	237
	0.8	1.391	14.87	7.20	7	420
	1.0	1.509	13.97	7.31	8	563
70.91	0.3	1.132	24.37	7.81	3	95
	0.5	1.234	22.88	9.17	4	169
	0.8	1.391	20.82	10.07	5	300
	1.0	1.509	19.55	10.24	6	403
101.3	0.3	1.132	34.81	11.15	2	67
	0.5	1.234	32.69	13.09	3	119
	0.8	1.391	29.75	14.39	4	211
	1.0	1.509	27.93	14.64	4	282

TABLE 2  
Absorption data for various  $C_{Bo}$  and  $P_A$  at 298 K

$P_A \times 10^{-2}$ (Pa)	$C_{Bo}$ (kmol/m <sup>3</sup> )	$\mu \times 10^3$ (kg/ms)	$C_{Ai} \times 10^4$ (kmol/m <sup>3</sup> )	$N_{A,exp} \times 10^7$ (kmol/m <sup>2</sup> s)	Hatta	$E_i$
10.13	0.3	1.008	3.12	1.24	25	728
	0.5	1.093	2.94	1.46	32	1296
	0.8	1.243	2.69	1.61	41	2294
	1.0	1.361	2.53	1.63	47	3069
30.39	0.3	1.008	9.35	3.70	8	243
	0.5	1.093	8.81	4.38	11	433
	0.8	1.243	8.06	4.82	14	765
	1.0	1.361	7.60	4.90	16	1024
50.65	0.3	1.008	15.58	6.17	5	147
	0.5	1.093	14.68	7.30	6	260
	0.8	1.243	13.44	8.04	8	460
	1.0	1.361	12.67	8.17	9	615
70.91	0.3	1.008	21.81	8.66	4	105
	0.5	1.093	20.56	10.21	5	186
	0.8	1.243	18.81	11.25	6	329
	1.0	1.361	17.73	11.44	7	440
101.3	0.3	1.008	31.15	12.53	2	74
	0.5	1.093	29.37	14.65	3	131
	0.8	1.243	26.88	16.08	4	231
	1.0	1.361	25.33	16.35	5	308

TABLE 3  
Absorption data for various  $C_{Bo}$  and  $P_A$  at 303 K

$P_A \times 10^{-2}$ (Pa)	$C_{Bo}$ (kmol/m <sup>3</sup> )	$\mu \times 10^3$ (kg/ms)	$C_{Ai} \times 10^4$ (kmol/m <sup>3</sup> )	$N_{A,exp} \times 10^7$ (kmol/m <sup>2</sup> s)	Hatta	$E_i$
10.13	0.3	0.901	2.80	1.35	28	806
	0.5	0.980	2.65	1.60	36	1430
	0.8	1.113	2.44	1.78	47	2517
	1.0	1.217	2.31	1.82	53	3355
30.39	0.3	0.901	8.39	4.05	9	270
	0.5	0.980	7.94	4.81	12	478
	0.8	1.113	7.31	5.33	16	840
	1.0	1.217	6.92	5.45	18	1119
50.65	0.3	0.901	13.99	6.75	6	162
	0.5	0.980	13.24	8.01	7	287
	0.8	1.113	12.19	8.88	9	504
	1.0	1.217	11.53	9.07	11	672
70.91	0.3	0.901	19.59	9.46	4	116
	0.5	0.980	18.54	11.21	5	205
	0.8	1.113	17.06	12.44	7	361
	1.0	1.217	16.15	12.71	8	480
101.3	0.3	0.901	27.98	13.61	3	82
	0.5	0.980	26.48	16.05	4	144
	0.8	1.113	24.38	17.76	5	253
	1.0	1.217	23.07	18.16	5	337

TABLE 4  
Absorption data for various  $C_{Bo}$  and  $P_A$  at 313 K

$P_A \times 10^{-2}$ (Pa)	$C_{Bo}$ (kmol/m <sup>3</sup> )	$\mu \times 10^3$ (kg/ms)	$C_{Ai} \times 10^4$ (kmol/m <sup>3</sup> )	$N_{A,exp} \times 10^7$ (kmol/m <sup>2</sup> s)	Hatta	$E_i$	
10.13	0.3	0.782	2.28	1.52	35	973	
	0.5	0.870	2.18	1.80	46	1717	
	0.8	0.986	2.03	2.02	59	2987	
	1.0	1.060	1.93	2.09	66	3943	
	30.39	0.3	0.782	6.85	4.55	12	325
	0.5	0.870	6.53	5.39	15	573	
	0.8	0.986	6.08	6.05	20	996	
	1.0	1.060	5.80	6.27	22	1315	
50.65	0.3	0.782	11.41	7.58	7	196	
	0.5	0.870	10.88	8.98	9	345	
	0.8	0.986	10.13	10.08	12	598	
	1.0	1.060	9.66	10.46	13	790	
70.91	0.3	0.782	15.98	10.61	5	140	
	0.5	0.870	15.24	12.58	7	246	
	0.8	0.986	14.19	14.13	8	428	
	1.0	1.060	13.53	14.63	9	564	
101.3	0.3	0.782	22.82	15.19	3	98	
	0.5	0.870	21.77	17.98	5	173	
	0.8	0.986	20.27	20.19	6	300	
	1.0	1.060	19.33	20.90	7	395	

where  $h_+$ ,  $h_-$  and  $h_{CO_2}$  are obtained as follows (19):

$$h_+ = 0.0922, h_- = 0.368 - 9.98 \times 10^{-4} T, \text{ and}$$

$$h_A = -0.0172 - 3.38 \times 10^{-4}(T - 298.15)$$

The Henry constant ( $H_{AW}$ ) of  $CO_2$  in water is obtained from the empirical equation (18):

$$H_{AW} = 2.8249 \times 10^9 \exp\left(-\frac{2044}{T}\right) \quad (25)$$

The solubility ( $C_{Ai}$ ) of  $CO_2$  of a given partial pressure of  $CO_2$  in aqueous solution of PT was estimated as follows:

$$P_A = H_A C_{Ai} \quad (26)$$

It is generally accepted that the diffusivity coefficient of a diffusant in solution can be related to the solution viscosity through modified Stokes-Einstein equation:

$$D_i \mu^\alpha = \text{constant} \quad (27)$$

where  $\alpha$  is a constant that depends on the diffusant/solvent.

$\alpha = 0.8$  can be considered to estimate  $D_A$  in the aqueous solution of PT and  $\alpha = 0.6$  to estimate  $D_B$  in solution (5).

Diffusivity of  $CO_2$  in water ( $D_{AW}$ ) is obtained from the empirical equation (18):

$$D_{AW} = 2.35 \times 10^{-6} \exp\left(-\frac{2119}{T}\right) \quad (28)$$

Diffusivity of PT in water ( $D_{BW}$ ) is obtained from Portugal et al. (5).

Viscosity of aqueous solution of PT was measured using Cannon-Fenske viscometer (Brookfield Eng. Lab. Inc, USA).

Viscosity and solubility at different  $C_{Bo}$ ,  $P_A$ , and  $T$  are listed in Tables 1–4.

## RESULTS AND DISCUSSION

The carbon dioxide absorption performance of PT at 1 kmol/m<sup>3</sup> and 298 K was compared to the absorption performance of diethanolamine (DEA), respectively, obtained using the same set-up and method. Results, shown in Fig. 2, confirm that although it is slower than DEA and PT by Portugal et al. (5), its absorption rates seem to be within the rates in these reference data.

$N_{A,exp}$ , listed in Tables 1–4, were used to investigate the reaction kinetics between  $CO_2$  and PT in the range of 0.3–1.0 kmol/m<sup>3</sup> of PT, 1.013–10.13 kPa of  $CO_2$  partial pressure, and 293–313 K.

To determine the order with respect to  $CO_2$  in the overall reaction (iv) between  $CO_2$  and PT, logarithmic plots of

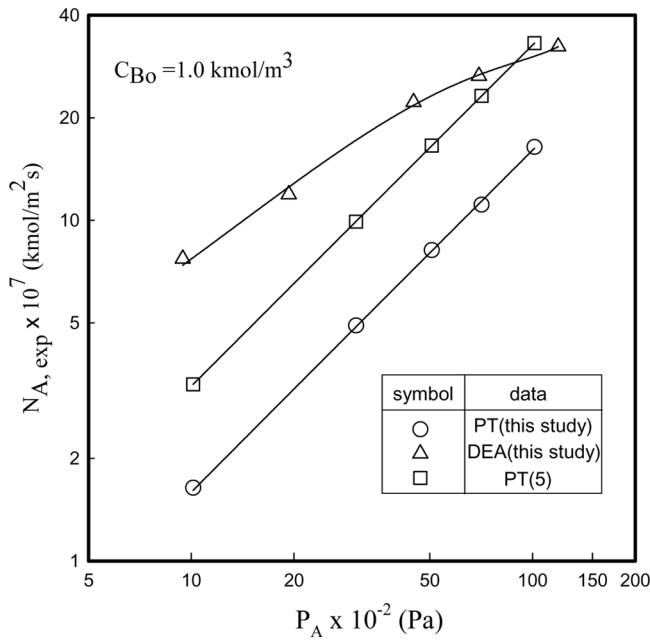


FIG. 2. Comparison of CO<sub>2</sub> flux in PT, DEA, and PT solution by Portugal et al. (5).

$N_{A,\text{exp}}$  vs.  $C_{Ai}$  are shown in Fig. 3 with typical  $C_{B0}$  of 1.0 kmol/m<sup>3</sup> and parameters of temperatures, and Fig. 4 with typical 298 K and parameters of  $C_{B0}$ .

The plots are linear with  $r^2 > 0.994$  and  $m$  from slopes approach to unity. These results were exhibited equally

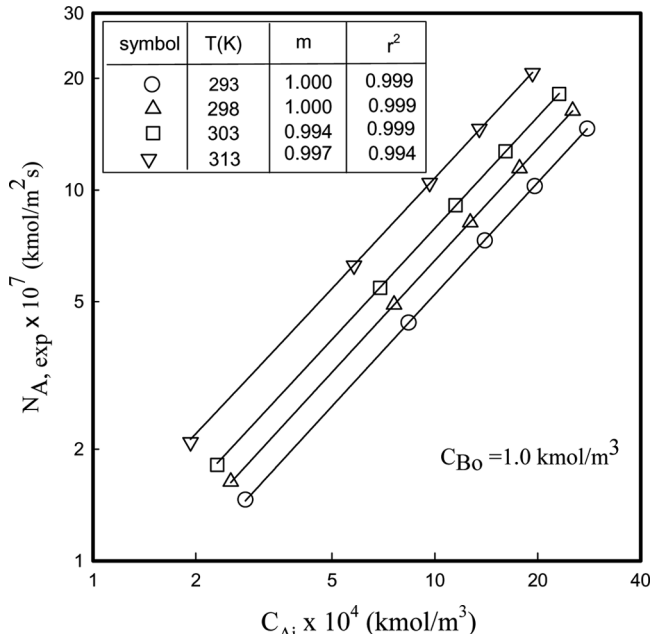


FIG. 3. Effect of  $C_{Ai}$  on  $N_{A,\text{exp}}$  at different temperatures at  $C_{B0} = 1.0 \text{ kmol/m}^3$ .

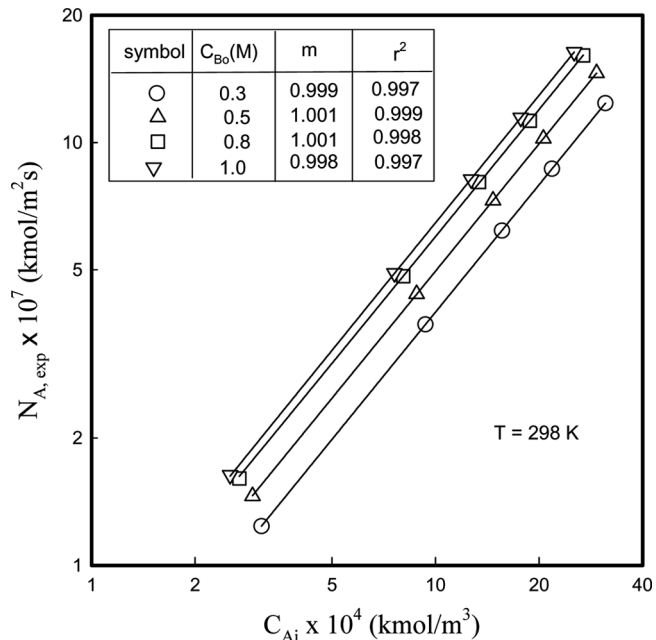


FIG. 4. Effect of  $C_{Ai}$  on  $N_{A,\text{exp}}$  at different concentrations at  $T = 298 \text{ K}$ .

for other conditions of  $C_{B0}$  and temperatures. According to Eq. (11) and these plots, the order with respect to CO<sub>2</sub> is 1.

To determine the order with respect to the concentration of PT,  $N_{A,\text{exp}}/(C_{Ai}D_A^{0.5})$  was plotted against  $C_{B0}$  at different  $C_{B0}$  of 0.3–1.0 kmol/m<sup>3</sup> in  $y_A$  of 0.01–0.1 and temperatures of 293–313 K. Logarithmic plots of  $N_{A,\text{exp}}/(C_{Ai}D_A^{0.5})$  vs.  $C_{B0}$  are shown in Fig. 5 with a typical  $y_A$  of 0.1 and parameters of temperatures.

Each of these plots is a straight line ( $r^2 > 0.998$ ), and  $n$  from slopes approach to unity and  $k$  are obtained from the intercept. The results for other  $y_A$  were exhibited equally. The values of  $k$  at each temperature are averaged using  $k$  of  $y_A$  and listed in Table 5.

Linear regression analysis of the Arrhenius plots, shown in Fig. 6, leads the following expression for  $k$  with  $r^2$  of 0.993.

$$k = 3.95 \times 10^9 \text{ Exp}(-4883/T) \quad (29)$$

The corresponding value of the activation energy ( $\Delta E_{A,\text{overall}}$ ) has been calculated to be 40.6 kJ/mol.

Portugal et al. (5) investigated the kinetics of the CO<sub>2</sub>-PT reaction using a stirred cell reactor in the fast pseudo-first-order reaction regime and flux was determined by the pressure drop method. They presented first order with respect to both CO<sub>2</sub> and PT, and the activation energy of 40.6 kJ/mol. The discrepancy is found not only in the activation energy but also in the experimental values of absorption rate as shown in Tables 1–4. The value of  $k$ , obtained from the intercept of the straight line of

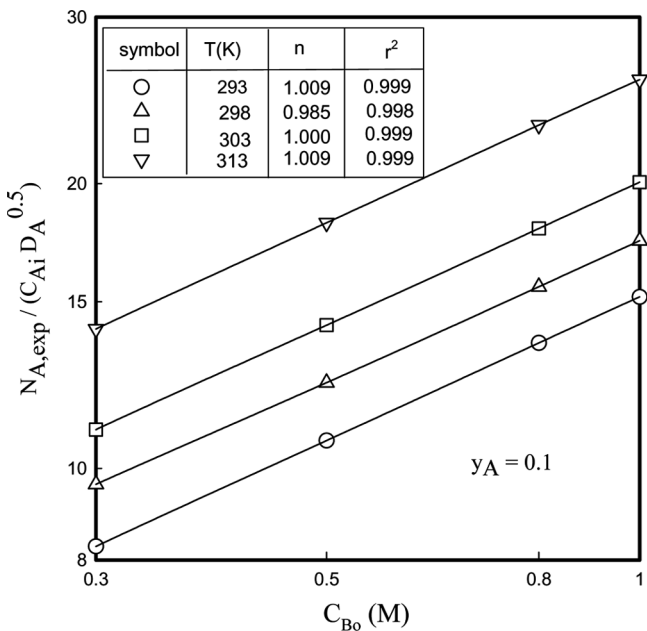


FIG. 5. Logarithmic plot of  $N_{Ae,exp} / (C_{Ai} D_A^{0.5})$  vs.  $C_{Bo}$  at different temperatures at  $y_A = 0.1$ .

logarithmic plots of  $N_{Ae,exp} / (C_{Ai} D_A^{0.5})$  vs.  $C_{Bo}$ , as shown in Fig. 5, is influenced by  $C_{Ai}$  and  $D_A$ . The discrepancy of these activation energies may, to some extent, be attributed to the uncertainties in the values of solubility and diffusivity of  $CO_2$ . The discrepancy of the experimental values of the absorption rate may be the differences of the gas/liquid contactor and analysis method about the rate data.

To ensure that the gas phase resistance was really negligible in all run, plots of  $P_A / N_{Ae}$  vs.  $H_A / (k D_A C_{Bo})^{0.5}$  at different  $y_A$ ,  $C_{Bo}$ , and temperatures have been made following Eq. (12) for  $m = 1$ ,  $n = 1$  using relevant data from Tables 1–4. The corresponding values of  $H_A$  and  $D_A$  have been estimated using Eqs. (23)–(28). These plots are presented in Fig. 7 at a typical  $y_A$  of 0.1.

It can be seen that all plots of  $P_A / N_{Ae,exp}$  vs.  $H_A / (k D_A C_{Bo})^{0.5}$  are straight lines with slope of 1 and passing through the origin. This, according to Eq. (12), signifies

TABLE 5  
Reaction rate constant for  $CO_2$  – PT reaction at different temperatures

T (K)	k ( $m^3/kmol \cdot s$ )	$k_1$ ( $m^3/kmol \cdot s$ )	$k_2/k_3 \times 10^3$ ( $kmol/m^3$ )
293	230.3	232.7	3.738
398	302.6	304.1	4.627
303	402.7	405.1	5.305
313	665.0	668.9	6.782

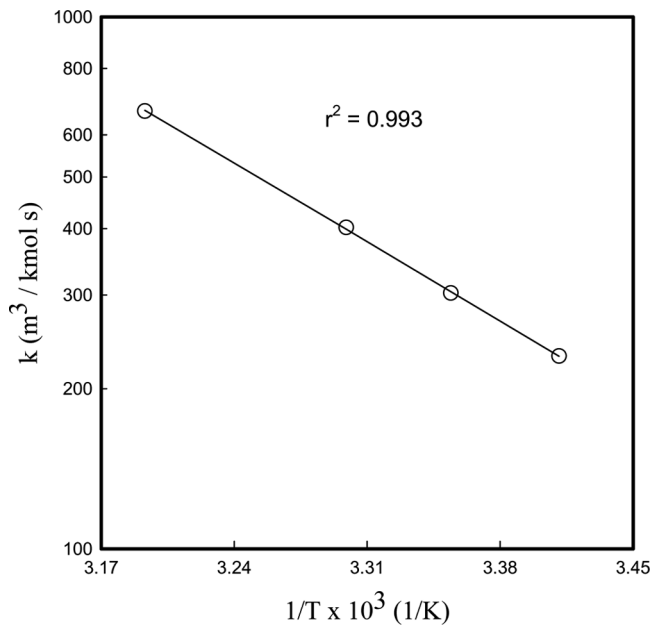


FIG. 6. Arrhenius plots of  $k$  for  $CO_2$ -PT reaction.

negligible gas phase resistance. The results are exhibited equally for other conditions of  $y_A$ .

To ensure that the reaction between  $CO_2$  and PT is a pseudo-first-order reaction regime, the concentrations of  $CO_2$  and PT in the liquid film are obtained from the numerical solution of Eqs. (1) and (2) with the boundary conditions of Eqs. (3) and (4) using the finite element

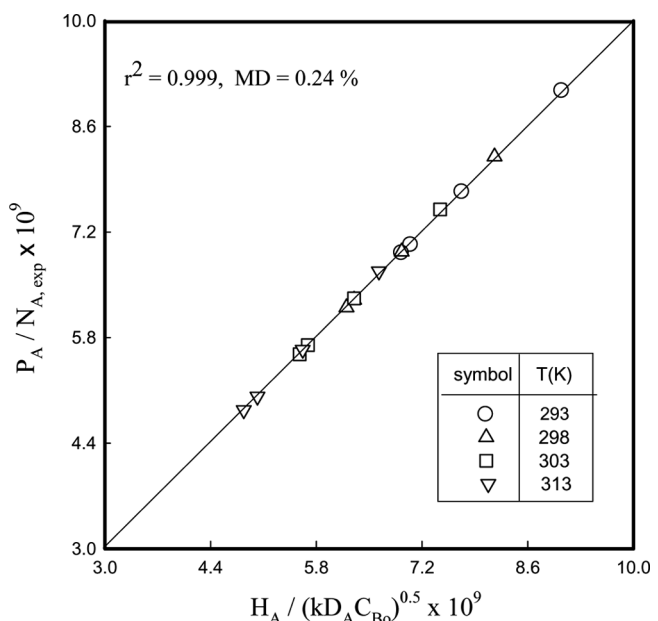


FIG. 7. Plots of  $P_A / N_{Ae}$  vs.  $H_A / (k D_A C_{Bo})^{0.5}$  at various temperatures and  $y_A = 0.1$ .

method by FEMLAB soft program with the values of  $k$ ,  $D_A$ ,  $D_B$ ,  $C_{Ai}$ , and  $k_L$ . At the typical condition of  $P_A = 10.13 \text{ kPa}$  and  $298 \text{ K}$ , the dimensionless concentration profiles of  $\text{CO}_2$  and PT in the liquid film are illustrated in Fig. 8 for  $C_{Bo}$  of  $0.5$  and  $1.0 \text{ kmol/m}^3$ , respectively.

$C_A$  decreases and  $C_B$  increases with increasing the depth of the liquid film, and the slope of the concentration profile of  $\text{CO}_2$  at the gas-liquid interface increase with increasing  $C_{Bo}$ , which make  $N_{A,\text{exp}}$  increased as shown in Tables 1–4. The values of  $C_B$  at the gas-liquid interface increase with increasing  $C_{Bo}$  and all of them are above  $0.97$ . This means that  $C_B$  may be constant as  $C_{Bo}$  at this typical condition. The values of Hatta and  $E_i$  at  $m=n=1$  are calculated by Eqs. (7) and (8), and listed in Tables 1–4. As shown Tables 1–4, Eq. (6) is satisfied. Therefore, the reaction between  $\text{CO}_2$  and PT is a fast pseudo-first-order reaction regime.

To obtain the elementary reaction kinetics based on the zwitterions mechanism of reaction (i) and (ii),  $k_o$  were obtained using  $\beta_{\text{exp}}$  and Eq. (22) in the range of  $0.3$ – $1.0 \text{ kmol/m}^3$  of PT for various  $y_A$  and temperatures. Plots of  $k_o$  against  $C_{Bo}$  are presented for various temperatures at a typical  $y_A$  of  $0.1$  in Fig. 9.

The plots satisfy a straight line, and  $k_o$  increase with increasing temperature and  $C_{Bo}$ .

Plots of  $C_{Bo}/k_o$  against  $1/C_{Bo}$  are presented in Fig. 10 for various temperatures at a typical  $y_A$  of  $0.1$ .

The plots satisfy a straight line, with the values of  $k_1$  and  $k_2/k_3$ , according to Eq. (22), obtained from the intercept

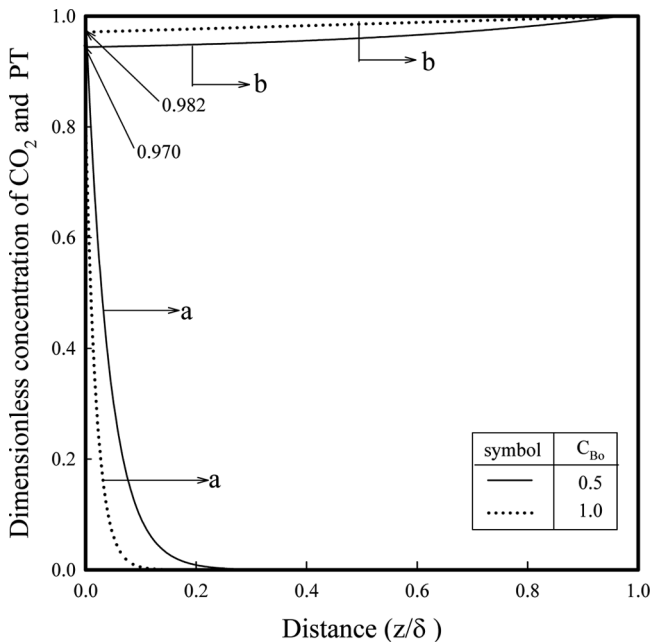


FIG. 8. Dimensionless concentration profiles of  $\text{CO}_2$  and PT in the liquid film at  $P_A = 10.13 \text{ kPa}$  and  $298 \text{ K}$  for different  $C_{Bo}$ . ( $a = C_A/C_{Ai}$ ,  $b = C_B/C_{Bo}$ ).

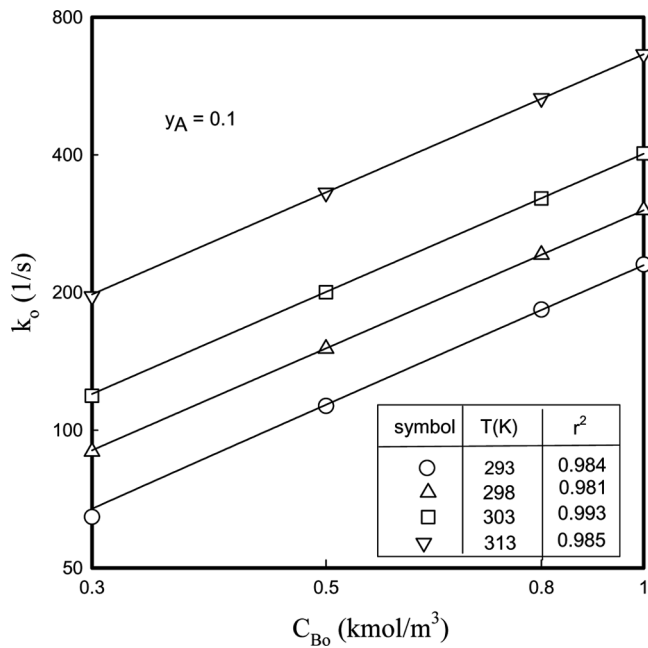


FIG. 9. Dependence of  $k_o$  on  $C_{Bo}$  at different temperature and  $y_A = 1.0$ .

and slope of the straight line, respectively. These results are exhibited equally at other  $y_A$ . The values of  $k_1$  and  $k_2/k_3$  for various temperatures are listed in Table 5 and give the Arrhenius plots of Fig. 11 and 12. The linear regression analysis of the Arrhenius plots in Fig. 11 gives  $40.5 \text{ kJ/mol}$  of the activation energy ( $\Delta E_{A,\text{elem}}$ ).

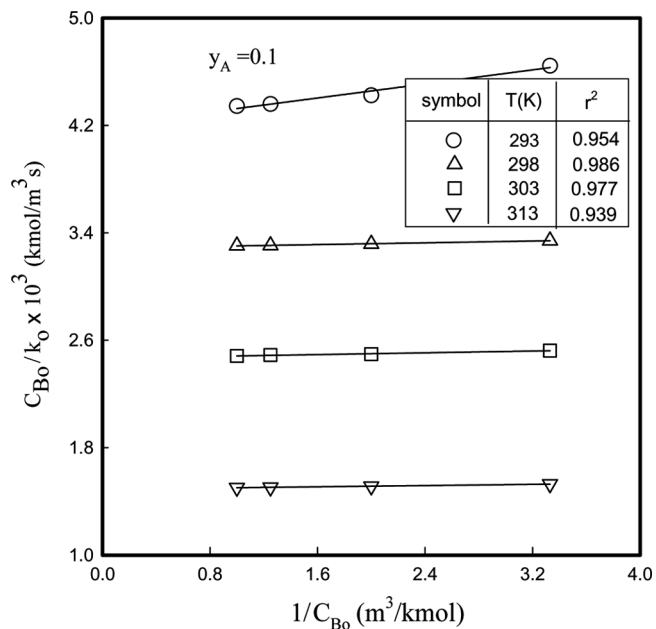
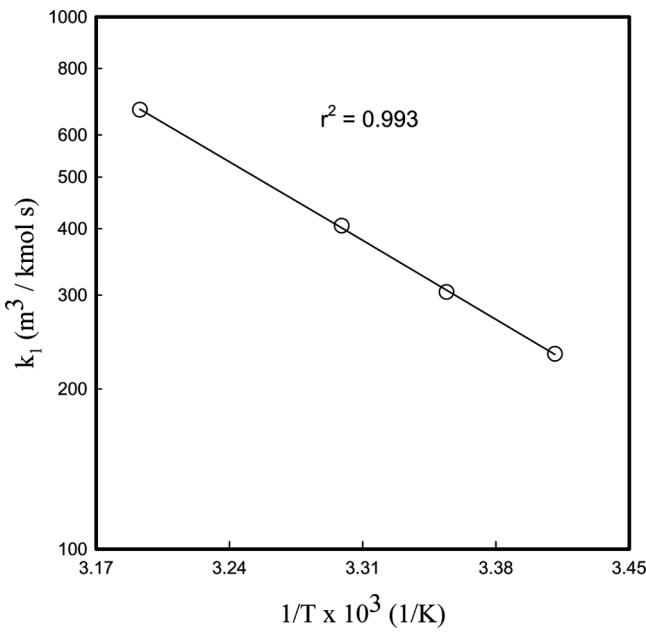
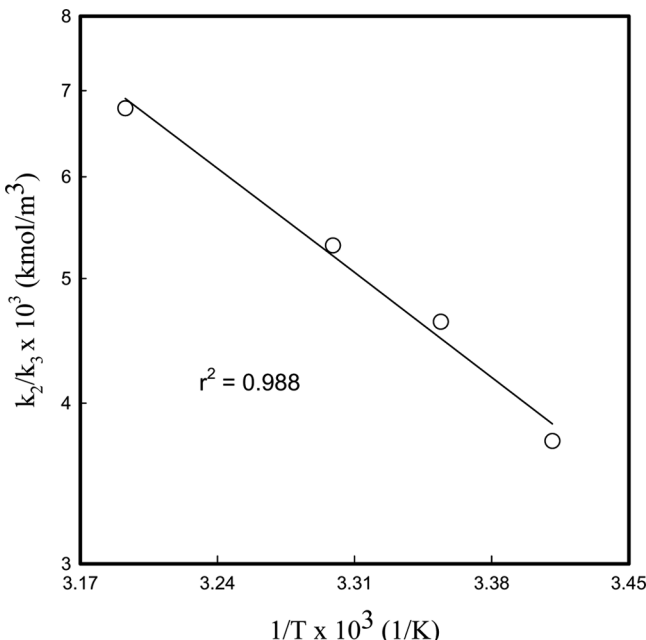
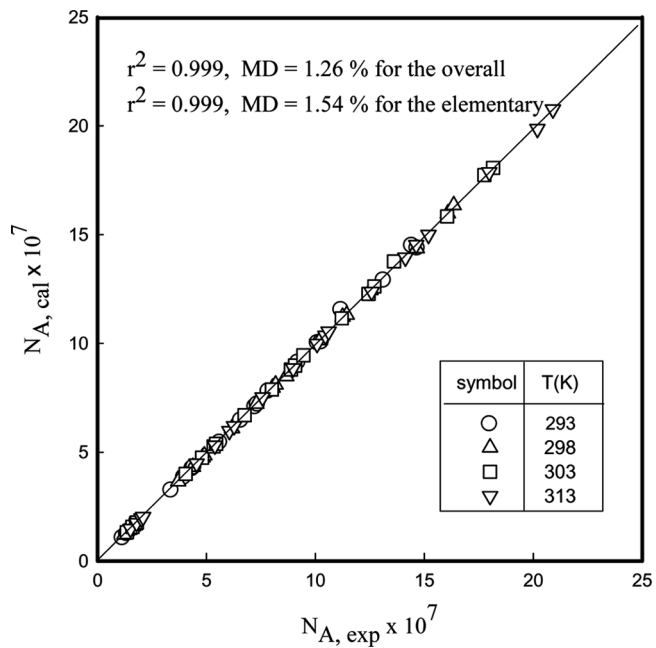


FIG. 10. Plots of  $C_{Bo}/k_o$  vs.  $1/C_{Bo}$  at different temperatures at  $y_A = 0.1$ .

FIG. 11. Arrhenius plot of  $k_1$ .

As shown in Table 5,  $k$  approaches to  $k_1$  and  $k_2/k_3$  is much less than 1, which ensures the assumption of an instantaneous reaction of reaction (ii) (6).

To compare the experimental fluxes of  $\text{CO}_2$  with theoretical ones, the theoretical fluxes are obtained by Eq. (5). The concentration gradient in Eq. (5) is estimated from the numerical solution of Eqs. (1) and (2) using  $k$  in the overall reaction scheme, and Eqs. (14) and (15) using of

FIG. 12. Arrhenius plot of  $k_2/k_3$ .FIG. 13. Comparison of estimated flux of  $\text{CO}_2$  with observed ones at different temperatures. ( $C_{\text{Bo}}$ : 0.3–1.0  $\text{kmol}/\text{m}^3$ ,  $P_{\text{A}}$ : 1.013–10.13  $\text{kPa}$ ).

$k_1$  and  $k_2/k_3$  in the elementary reaction scheme, respectively. The observed and estimated fluxes for both the reaction kinetics are shown in Fig. 13 in  $C_{\text{Bo}}$  of 0.3–1.0  $\text{kmol}/\text{m}^3$ , 1.013–10.13  $\text{kPa}$  of  $\text{CO}_2$  partial pressure, and 293–313 K.

As shown in Fig. 13, the observed fluxes agree very well with the estimated values with  $r^2$  of 0.999, MD of 1.26% for the overall reaction scheme, and  $r^2$  of 0.999, MD of 1.54% for the elementary reaction scheme.

From the results mentioned above, i.e., the same values, such as  $k$  and  $k_1$ ,  $\Delta E_{\text{A,overall}}$  and  $\Delta E_{\text{A,elem}}$ , and the statistics in Fig. 13, it was concluded that the overall reaction (iii) becomes to be equivalent to the forward reaction (i), i.e., the formation of zwitterions.

## CONCLUSIONS

The reaction kinetics between  $\text{CO}_2$  and PT has been interpreted by the overall reaction scheme and the elementary reaction scheme in the range of 293–313 K using a stirred semi-batch vessel with a planar gas-liquid interface. Both the reaction order and rate constant in the overall reaction scheme were determined from gas absorption rates under the fast pseudo-first-reaction regime. Its reaction was found to be first order with respect to both  $\text{CO}_2$  and PT, and the activation energy has been found to be 40.6  $\text{kJ}/\text{mol}$ . From a comparison of the reaction kinetics by the overall reaction scheme with those by the elementary reaction scheme based on the zwitterions mechanism, the overall reaction between  $\text{CO}_2$  and PT has been found to

be equivalent to the formation of zwitterions. The experimental absorption rates approached very well to the theoretical values based on the film theory with the overall reaction scheme and the elementary reaction scheme, respectively.

## NOMENCLATURE

$C_i$	concentration of species, $i$ (kmol/m <sup>3</sup> )
$D_i$	diffusivity of species, $i$ (m <sup>2</sup> /s)
$E_i$	instantaneous reaction enhancement factor define in Eq. (8)
Hatta	Hatta number defined in Eq. (7)
$H_A$	Henry constant of CO <sub>2</sub> (m <sup>3</sup> · kPa/kmol)
$k_G$	gas phase mass transfer coefficient of CO <sub>2</sub> (m <sup>2</sup> · s · kPa/kmol)
$k_L$	liquid-side mass transfer coefficient of CO <sub>2</sub> in absorbent (m/s)
$k_m$	pseudo mth order reaction rate constant in Eq. (10) (1/s)
$k$	second-order reaction rate constant in reaction (iv) (m <sup>3</sup> /kmol · s)
$k_1$	forward reaction rate constant in reaction (i) (m <sup>3</sup> /kmol · s)
$k_2$	backward reaction rate constant in reaction (i) (1/s)
$k_3$	reaction rate constant in reaction (ii) (m <sup>3</sup> /kmol · s)
$k_o$	pseudo-first-order reaction rate constant (1/s)
$m$	reaction order with respect to CO <sub>2</sub>
$n$	reaction order with respect to PT
$P_A$	partial pressure of CO <sub>2</sub> (Pa)
PT	potassium threonate
$N_A$	molar flux of CO <sub>2</sub> defined in Eq. (5) (kmol/m <sup>2</sup> · s)
$N_{A,exp}$	experimental molar flux of CO <sub>2</sub> (kmol/m <sup>2</sup> · s)
$r^2$	correlation coefficient
$r_{A1}$	pseudo-first-order reaction rate defined in Eq. (16)
$r_{A,overall}$	reaction rate defined in Eq. (v)
$r_{A,elemen}$	reaction rate defined in Eq. (13)
T	temperature (K)
z	diffusion coordinate of CO <sub>2</sub> (m)

## Greek Letters

$\beta$	enhancement factor of CO <sub>2</sub> by the chemical reaction
$\delta$	liquid film thickness (m)
$\nu_A$	a stoichiometric coefficient of species A

## Subscripts

A	CO <sub>2</sub>
B	PT
i	gas-liquid interface
o	feed

## ACKNOWLEDGEMENTS

This work was supported by Brain Korea 21 Project and a grant (2006-C-CD-11-P-03-0-000-2007) from the Energy Technology R&D of Korea Energy Management Corporation. Dae-Won Park is also thankful for KOSEF (R01-2007-000-10183-0).

## REFERENCES

1. Aboudheir, A.; Totiwachwuthikul, P.; Chkma, A. (2003) Kinetics of the reactive absorption of carbon dioxide in high-loaded concentrated aqueous monoethanolamine solutions. *Chem. Sci. Eng.*, 50: 1071–1079.
2. Ali, S.H. (2005) Kinetics of the reaction of carbon dioxide with blends of amines in aqueous media using the stopped-flow technique. *J. Chem. Kinet.*, 37: 391–405.
3. Paul, S.; Ghoshal, A.K.; Mandal, B. (2009) Kinetics of absorption of carbon dioxide into aqueous blends of 2-(1-piperazinyl)-ethylamine and N-methyldiethanolamine. *Chem. Sci. Eng.*, 64: 1618–1622.
4. Park, S.W.; Park, D.W.; Oh, K.J.; Kim, S.S. (2009) Simultaneous absorption of carbon dioxide and sulfur dioxide into aqueous 2-amino-2-methyl-1-propanol. *Sep. Sci. Technol.*, 44: 543–568.
5. Portugal, A.F.; Magalhaes, F.D.; Mendes, A. (2008) Carbon dioxide absorption kinetics in potassium threonate. *Chem. Eng. Sci.*, 63: 3493–3503.
6. Holst, J.; Politiek, P.P.; Niederer, J.P.M.; Versteeg, G.F. (2006) CO<sub>2</sub> capture from flue gas using amino acid salts solutions. GHGT-8 Proceedings, Norway.
7. Kumar, P.S.; Hogendoorn, J.A.; Feron, P.H.M.; Versteeg, G.F. (2001) Density, viscosity, solubility, and diffusivity of N<sub>2</sub>O in aqueous amino acid salt solution. *J. Chem. Eng. Data*, 46: 1357–1361.
8. Kohl, A.L.; Nielson, R.B. (1997) *Gas Purification*; Gulf Publishing: Houston.
9. Chen, H.; Kovvali, A.S.; Sirkar, K.K. (2000) Selective CO<sub>2</sub> separation from CO<sub>2</sub>-N<sub>2</sub> mixtures by immobilized glycine-Na-glycerol membranes. *Ind. Eng. Chem. Res.*, 39: 2447–2451.
10. Lee, S.; Song, H.J.; Maken, S.; Park, J.W. (2007) Kinetics of CO<sub>2</sub> absorption in aqueous sodium glycinate solutions. *Ind. Eng. Chem. Res.*, 46: 1578–1583.
11. Park, S.W.; Son, Y.S.; Park, D.W.; Oh, K.J. (2008) Absorption of carbon dioxide into aqueous solution of sodium glycinate. *Sep. Sci. Technol.*, 43: 3003–3019.
12. Portugal, A.F.; Sousa, J.M.; Magalhaes, F.D.; Mendes, A. (2009) Solubility of carbon dioxide in aqueous solutions of amino acid salts. *Chem. Eng. Sci.*, 64: 1993–2002.
13. Danckwerts, P.V. (1979) The reaction of CO<sub>2</sub> in ethanolamines. *Chem. Eng. Sci.*, 34: 443–446.
14. Daraishwary, L.K.; Sharma, M.M. (1984) *Heterogeneous Reaction: Analysis, Example and Reactor Design*; John Wiley & Sons: New York.
15. Caplow, M. (1968) Kinetics of carbamate formation and breakdown. *J. Am. Chem. Soc.*, 90: 6795–6803.
16. da Silva, E.F.; Sendsen, H.F. (2004) An initial study of the reaction of carbamate formation from CO<sub>2</sub> and alkanolamine. *Ind. Eng. Chem. Res.*, 43: 3413–3418.
17. Yu, W.C.; Astarita, G.; Savage, D.W. (1985) Kinetics of carbon dioxide absorption in solutions of methyldiethanolamine. *Chem. Eng. Sci.*, 40: 1585–1590.
18. Versteeg, G.F.; van Swaaij, W.P.M. (1988) Solubility and diffusivity of acids gases (CO<sub>2</sub>, N<sub>2</sub>O) in aqueous alkanolamine solutions. *J. Chem. Eng. Data*, 33: 29–34.
19. Weisenberger, S.W.; Schumpe, A. (1996) Estimation of gas solubility in salt solutions at temperatures from 273 K to 363 K. *AIChE J.*, 42: 298–300.
20. Danckwerts, P. V. (1970) *Gas-Liquid Reactions*; McGraw-Hill Book Comp.: New York.